Gastric Cancer (2020) 23:241–259
https://doi.org/10.1007/s10120-019-01004-z

ORIGINAL ARTICLE

The modification of ferroptosis and abnormal lipometabolism through overexpression and knockdown of potential prognostic biomarker perilipin2 in gastric carcinoma

Xiaoying Sun[1,2] · Shaojuan Yang[2,3] · Xuechao Feng[4] · Yaowu Zheng[4,5] · Jinsong Zhou[1,2] · Hai Wang[1,2] · Yucheng Zhang[2,6] · Hongyan Sun[2,7] · Chengyan He[1,2]

Received: 23 June 2019 / Accepted: 2 September 2019 / Published online: 13 September 2019

Abstract

Background To investigate the biological relationship, mechanism between perilipin2 and the occurrence, advancement of gastric carcinoma, and explore the mechanism of lipid metabolism disorder leading to gastric neoplasm, and propose that perilipin2 is presumably considered as a potential molecular biomarker of gastric carcinoma.

Methods RNA-seq was applied to analyze perilipin2 and differentially expressed genes modulated by perilipin2 in neoplastic tissues of both perilipin2 overexpression and knockdown groups in vivo. The mechanism was discovered and confirmed by Rt-qPCR, immunoblotting, immunohistochemistry, staining and microassay, respectively. Cellular function experiments were performed by flow cytometry, CCK8, clonogenic assay, etc.

Results Overexpression and knockdown of perilipin2 augmented the proliferation and apoptosis of gastric carcinoma cell lines SGC7901 and MGC803, respectively. The neoplastic cells with perilipin2-overexpression obtained more conspicuously rapid growth than knockdown group in vivo, and perilipin2 affected the proliferation and apoptosis of gastric carcinoma cells by modulating the related genes:acyl-coa synthetase long-chain family member 3, arachidonate 15-lipoxygenase, microtubule associated protein 1 light chain 3 alpha, pr/set domain 11 and importin 7 that were participated in Ferroptosis pathway. Moreover, RNA-seq indicated perilipin2 was an indispensable gene and protein in the suppression of Ferroptosis caused by abnormal lipometabolism in gastric carcinoma.

Conclusion Our study expounded the facilitation of perilipin2 in regulating the proliferation and apoptosis of gastric carcinoma cells by modification in Ferroptosis pathway, and we interpreted that the mechanism of gastric neoplasm caused by obesity, we also discovered that pr/set domain 11 and importin 7 are novel transcription factors relevant to gastric carcinoma. Furthermore, perilipin2 probably serves not only as a diagnostic biomarker, but also a new therapeutic target.

Keywords Perilipin2 · Gastric carcinoma · Overexpression · Knockdown · Ferroptosis pathway · Lipometabolism

Electronic supplementary material The online version of this article (https://doi.org/10.1007/s10120-019-01004-z) contains supplementary material, which is available to authorized users.

✉ Xiaoying Sun
sun_xy@jlu.edu.cn

✉ Chengyan He
cyhe@jlu.edu.cn

[1] Department of Laboratory Medicine, China-Japan Union Hospital of Jilin University, Changchun 130033, China

[2] Norman Bethune Health Science Center of Jilin University, Changchun 130021, China

[3] Department of Pathology, China-Japan Union Hospital of Jilin University, Changchun 130033, China

[4] College of Life Sciences, Northeast Normal University, Changchun 130024, China

[5] Institute of Cardiovascular Research, University of California, San Francisco, CA 94101, USA

[6] Department of Science Research Center, China-Japan Union Hospital of Jilin University, Changchun 130033, China

[7] Department of Tissue Bank, China-Japan Union Hospital of Jilin University, Changchun 130033, China

Introduction

Gastric carcinoma is a foremost cause of mortality due to neoplastic disease [1], and the primitively definite diagnosis is still inadequate. Therefore, it is imperative to study the pathogenesis of gastric neoplasm. The significance of fatty acid metabolism in cancer initiation is increasingly accepted by the public due to the high prevalence of overweight individuals [2]. Some studies have exhibited that gastric cancer is associated with lipid accumulation [3]. Perilipin2 (PLIN2) is also known as adipose differentiation-related protein (ADRP), which belongs from PLIN, ADRP and the tail-interacting protein (PAT) family of cytoplasmic lipid droplet binding protein [4]. This protein surrounds the lipid droplet along with phospholipids and are involved in assisting the storage of neutral lipids within the lipid droplets [5]. Besides, Studies have reported that PLIN2 is significantly over-expressed in gastric cancer tissues by immunohistochemistry (IHC), PLIN2 was highly expressed in 79% category 3 cases of gastric epithelial neoplasia, and there was a stepwise increase in cryptal staining of PLIN2 from category 3 to category 5 [6]. However, few research has been implemented on specific mechanism that PLIN2 causes the gastric tumorigenesis by imbalanced lipid metabolism. Hence, we studied the mechanism of PLIN2 related to the emergence of gastric cancer including the effects of PLIN2 overexpression and knockdown on gastric cancer cell lines SGC7901 and MGC803 in vitro and the regulation of the principal genes in vivo to demonstrate the primacy of PLIN2 in the initiation of gastric neoplasm as a potential molecular biomarker. Additionally, one of the key challenges in cancer research is how to effectively kill cancer cells while leaving the healthy cells intact. Cancer cells often have defects in cell death executioner mechanisms, which is one of the main reasons for therapy resistance [7]. Ferroptosis is a recently recognized cell death modality that is morphologically, biochemically and genetically emerged to play an important role in cancer biology [8]. It has been reported that Ferroptosis can interfere with the development of diseases by activating or inhibiting iron death, which is related to Parkinson's syndrome [9], pancreatic cancer [10] and other diseases. Actually, we firstly presented that the impact of PLIN2 on Ferroptosis pathway as an oncogene and explained how the obesity can cause gastric cancer in this study.

Methods

Materials

Human gastric cancer cell lines SGC7901 and MGC803 were obtained as a gift from Bethune Second Clinical Medical College of Jilin University. The culture medium was RPMI 1640 (Invitrogen, the USA) and 10% FBS (Gibco, the USA) All cells were cultured in Incubator at 37 °C with 5% CO_2.

Overexpression and knockdown of PLIN2 transfection into SGC7901 and MGC803 cell lines

PLIN2 overexpression and knockdown plasmids were constructed by Sangong Biotechnology (Shanghai) Co., Ltd., the green fluorescent protein (GFP) in the plasmid as the indicator. The stable transfected cell lines were screened with limited dilution method after transfected by Lipo2000 (Invitrogen). The three different knockdown sites sense sequences of human were: Sh/SiPLIN2.1 GCTAGAGCC GCAAATTGCAGT, Sh/SiPLIN2.2 GTGTATAGTGCC AATCAGAAA, Sh/SiPLIN2.3GGAGCATTGGATATG ATGATA. Two control groups: OvCtrl and Sh/SiCtrl were transfected with empty vector pEGFP-N1 and pSGU6/GFP/Neo. The non-treatment control cells were classified as NC.

Cell proliferation and clonogenic assay

On day 0, 5000 cells were contained per well with 96-well plate for each day and six repeated wells were arranged in each group. Photographs were taken under fluorescence microscope from day 1 to day 5, respectively. Absorption values were measured 2 h after adding CCK8 reagent (MCE, the USA). The optical density (OD) was measured at 450 nm.

The transfected cells were replated on the 6-well plates at 1000 cells/well, and cultured in complete medium for about 2 weeks. Cells were then stained with crystal violet and individual colonies (> 50 cells) were counted.

Flow cytometry for detection of apoptosis in SGC7901 cell line

5×10^6 cells in each group were evenly spread on 10 cm dishes with PBS added to induce apoptosis for 48 h, the cells were digested and blended with Annexin V-PE (Apoptosis Detection Kit, Beyotime, China), the apoptotic rate was detected by flow cytometry (Beckman Cytomics FC 500, the USA).

Detection of apoptosis in MGC803 cell by fluorescence microscopy

$2–3 \times 10^6$ cells were cultured in 6 cm dishes in each group for 48 h of PBS-induced apoptosis, the apoptotic cells was counted in counting plate with adding 5 ml Annexin V-PE by fluorescence microscope.

Survival of PLIN2-overexpression and knockdown in SGC7901 and MGC803 cell lines

On day 0.3×10^6 cells were contained in 6 cm dishes in each group for each day. After 5 ml PBS was added to each well for FBS-free culture, the mortal cells were removed after 3 times of PBS rinsing for four consecutive days, and the survival cells were digested and counted.

Subcutaneous xenografts in vivo

All the animals in the experiment were treated gently and conformed to human ethical standards and international conventions. SGC7901 cell line transfected with OvPLIN2, ShPLIN2 and Control were injected subcutaneously into the nude mice (BALB/c nu/nu, female, 5 weeks old, Beijing Huafukang Biotechnology Co. Ltd. China) which were anaesthetized with 1% Sodium pentobarbital. The long diameter a and short diameter b of mouse tumor and the weights were measured every 4–5 days, and the relative tumor volumes (RTV) were calculated according to formula $0.5 \times a \times b \times b$. Body length of mice were also measured as the distance from nasal tip to anus. Mice were euthanized when long diameter reached 20 mm corresponding with our institutional guidelines for animal Ethics.

RNA-seq analysis

Xenografts were sent to The Beijing Genomics Institute (BGI, China). The purified total RNA was treated by RNA enrichment method after it was extracted by Magnetic bead method, RNA was subjected to RNA-Seq analysis on BGISEQ-500 system after the retranscription and qualification. Quantitative analysis of genes, based on gene expression level and enrichment analysis of GO functional and Pathway Significance Enrichment Analysis, Clustering, etc. among the selected samples after the comparison to reference genome.

Reverse transcription and quantitative real-time PCR (RT-qPCR)

Both total RNA from xenografts and cells were extracted by RNA Extraction Kit (Beyotime, China). Reverse transcription and qRT-PCR were performed according to Instruction of PrimeScript™ RT.

reagent Kit with gDNA Eraser for Perfect Real Time and TB Green™ Premix Ex Taq™ II (Takara, China), respectively. Primers for PLIN2: Forward TCAACTCAGATT GTTGCCAATG, Reverse TTTGGTGAGTGCATTTTC TACG. Primers for ACSL3: Forward CGTGTCTTCAAA ACCATCTACC, Reverse TCTTGTCTTGACTCGGAG AAAA. Primers for ALOX15: Forward TCACCTTCCTGC TCGCCTAGTG, Reverse GGTGCTGCTGGCTACAGA GAATG. Primers for LC3A: Forward CCTGGACAAGAC CAAGTTTTTG, Reverse GTAGACCATATAGAGGAA GCCG. Primers for IPO7: Forward GGCACATCCGCA CCGTCTTC, Reverse CGGACCGCATTCAGATCCTTC. Primers for PRDM11: Forward AAGAACAACCGCTAT AAGTCCA, Reverse GAGAACTTGGGCTTCCTCTTAC. The whole process was implemented by Applied Biosystems 7500 (the USA).

Immunoblotting

Immunoblotting was completed by the equipment (Bio-Rad, the USA). Cells and tissue were lysed in the intense radio-immunoprecipitation assay (RIPA) buffer with 1 mm PMSF (Beyotime, China) and 40 ul Protease Inhibitor Cocktail(cOmplete, Sigma, Germany) for 1 ml RIPA, quantified by BCA Protein Assay Kit (Signalway, the USA). Equivalent proteins were separated by 8%, 10%, 12% sodium dodecyl sulfate-polyacrylamide gel electrophoresis and electro-transferred to nitrocellulose membranes (Millipore, the USA). Membranes were blocked with PBST buffer containing 5% degreased milk and 0.1%.

Tween overnight at 4 °C and incubated for 2 h at room temperature with primary antibodies including PLIN2 (#ab201721Abcam, the USA), ACSL3 (#ab151959, Abcam, the USA), AlOX15 (#ab119774, Abcam, the USA), LC3A (#49049, Signalway, the USA), PRDM11 (#OM218595, Omni, the USA), IPO7 (#37658, Signalway, the USA), actin (#TA811000, ORIGENE, the USA), respectively. Actin was utilized as an internal control for loading control. The immunoblots were displayed with ECL (Thermo) after incubated with corresponding secondary antibodies (#L3012-2, Signalway, the USA).

The hematoxylin–eosin (HE) staining and immunohistochemistry (IHC)

Xenografts were fixed in 4% Paraformaldehyde, embedded in paraffin, and then cut into 4 μm thick sections for HE staining, the sections from the distilled water were placed in an aqueous solution of hematoxylin for several minutes, resolved eosin staining for 2–3 min. For IHC staining, slides were incubated with PLIN2 antibody (#OM270183, Omni, the USA) ACSL3 (#ab151959, Abcam, the USA), AlOX15 (#ab119774, Abcam, the USA), L C3A (#49049, Signalway, the USA), PRDM11 (#OM218595, Omni, the USA), IPO7

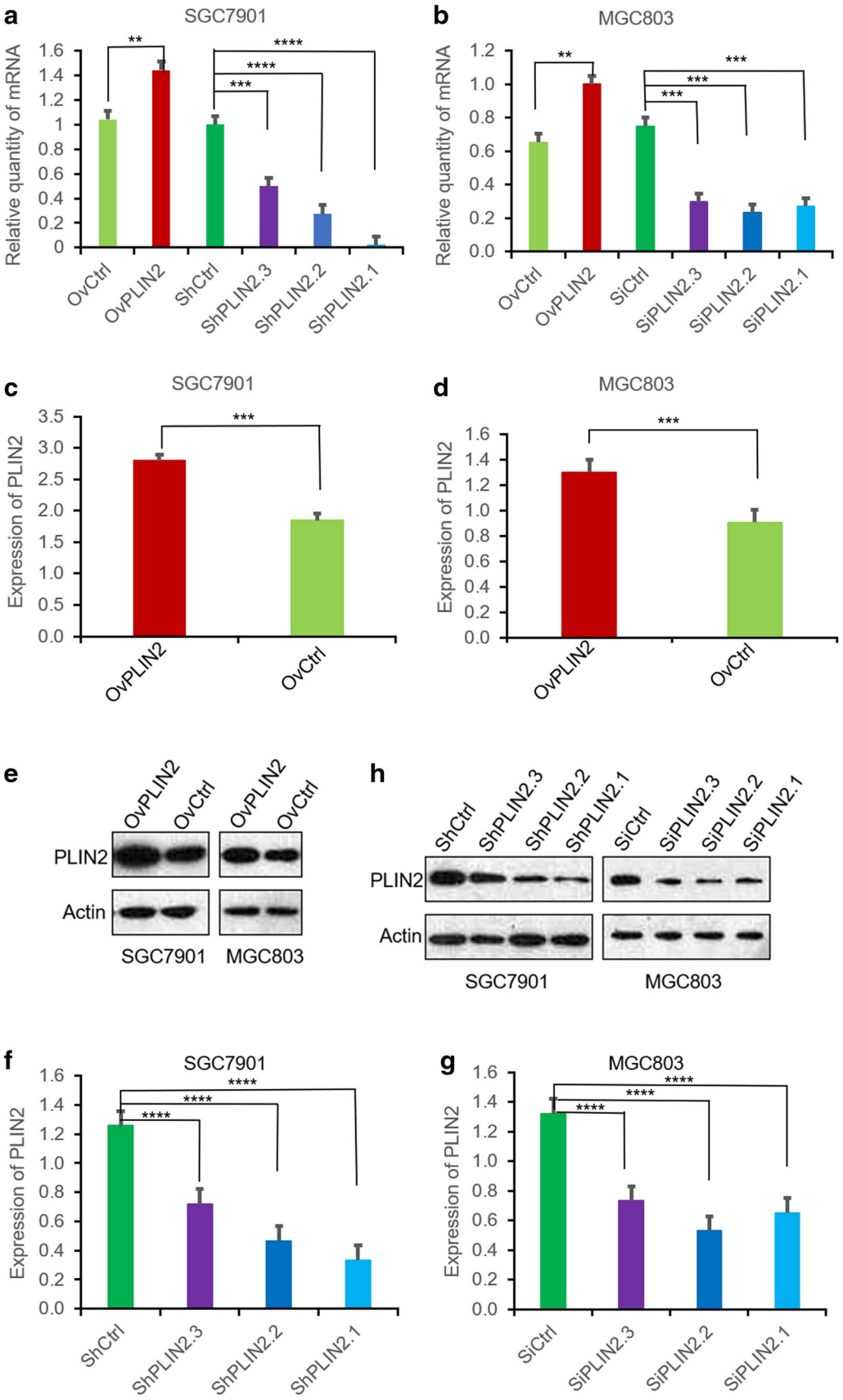
a
SGC7901
Relative quantity of mRNA
OvCtrl
OvPLIN2
ShCtrl
ShPLIN2.3
ShPLIN2.2
ShPLIN2.1
b
MGC803
Relative quantity of mRNA
OvCtrl
OvPLIN2
SiCtrl
SiPLIN2.3
SiPLIN2.2
SiPLIN2.1
c
SGC7901
Expression of PLIN2
OvPLIN2
OvCtrl
d
MGC803
Expression of PLIN2
OvPLIN2
OvCtrl
e
OvPLIN2
OvCtrl
OvPLIN2
OvCtrl
PLIN2
Actin
SGC7901
MGC803
h
ShCtrl
ShPLIN2.3
ShPLIN2.2
ShPLIN2.1
SiCtrl
SiPLIN2.3
SiPLIN2.2
SiPLIN2.1
PLIN2
Actin
SGC7901
MGC803
f
SGC7901
Expression of PLIN2
ShCtrl
ShPLIN2.3
ShPLIN2.2
ShPLIN2.1
g
MGC803
Expression of PLIN2
SiCtrl
SiPLIN2.3
SiPLIN2.2
SiPLIN2.1

◂**Fig. 1** Level of PLIN2 is heightened and declined after overexpression and knockdown of PLIN2 in SGC7901 and MGC803 cell lines. **a**, **b** Relative quantity of PLIN2 mRNA level was determined by Rt-qPCR in SGC7901 and MGC803 cell lines with overexpression and knockdown of PLIN2. **c**, **d** Level of PLIN2 protein was significantly enhanced after PLIN2 overexpressed transfection. **f**, **g** Level of PLIN2 protein was obviously decreased after PLIN2 knockdown transfection. **e**, **h** Immunoblotting for PLIN2 expression, Actin was loading control. $^{**}P<0.01$; $^{***}P<0.001$; $^{****}P<0.0001$

(#37658, Signalway, the USA) for 24 h at 4 °C after antigen retrieval and blocked with Non-immune goat serum and then incubated with secondary antibody at 25 °C for 30 min. Statistical analysis and IOD/area (mean density) for scoring by software IPP6.0.

Reactive oxygen species (ROS) generation assay

The ROS levels in the cells were determined by the Reactive Oxygen Species Assay Kit (Beyotime, China) according to the manufacturer's instructions. The cells were plated in triplicates (2×10^4 cells/well) and stimulated with medium containing 10 μM DCFH-DA for 30 min at 37 °C and washed by serum-free medium. The fluorescence intensity was monitored with excitation wavelength of 488 nm and at an emission wavelength of 535 nm by BioTek Instruments (the USA).

Nile red and Hoechst33342 fluorescence staining

The cells were plated in triplicates (3×10^4 cells/well) and fixed by 4% paraformaldehyde for 20 min. Each well was incubated for 10 min with 100 μl/well Nile Red working fluid (Abmole, the USA) at 37 °C of light avoidance. Washed with PBS for twice, stained with Hoechst33342 (Abmole, the USA) 100 μl/well at room temperature for 30 min. The fluorescence intensity and absorbance imaging of Nile Red and Hoechst33342 was at 552/636 nm and 353/483 nm.

Triglyceride microassay and Lee's Index evaluation of mice

The triglyceride levels of mouse tumor were determined by the Triglyceride Microassay Kit (Solarbio, China) according to the manufacturer's instructions. 0.1 g of mouse tumor tissue was added with 1 ml of n-heptane and isopropanol mixture, centrifuged with 8000*g* at 4 °C after ice bath homogenate. The OD value was measured at 420 nm. The body size was evaluated by Lee's Index = Body weight $1/2\times10^3$/Body length.

Results

The level of PLIN2 is heightened and declined after overexpression and knockdown of PLIN2 in SGC7901 and MGC803 cell lines

After 2–3 months of continuous culture, the stable transfection of over-expressed PLIN2 (OvPLIN2) and knockdown PLIN2 (ShPLIN2) into SGC7901 with 100% transfection efficiency. For MGC803, the stable transfection efficiency of OvPLIN2 and SiPLIN2 were 100% and over 90%, respectively. The level of over-expressed of PLIN2 in SGC7901, MGC803 and knockdown of ShPLIN2.1, 2, 3 in SGC7901, SiRNA1, 2, 3 of PLIN2 in MGC803 were confirmed by Rt-qPCR (Fig. 1a, b) and immunoblotting, respectively (Fig. 1e, h). Both Rt-qPCR and immunoblotting results showed that OvPLIN2 expressed higher PLIN2 level than OvCtrl in SGC7901 (Fig. 1a, c) and MGC803 (Fig. 1b, d). Oppositely, ShPLIN2 in SGC7901 and SiRNA of PLIN2 in MGC803 expressed lower PLIN2 level than the control groups ShCtrl (Fig. 1a, f), SiCtrl (Fig. 1b, g).

Cell proliferation is accelerated and attenuated with enhancement and suppression of PLIN2

Compared with the OvCtrl, proliferative rate of SGC7901 cells in OvPLIN2 increased prominently (Fig. 2a, b), while it strikingly decreased in ShPLIN2.1, ShPLIN2.2 and ShPLIN2.3 after gene PLIN2 was knockdown at three different sites, ShPLIN2.1 was the most effective in inhibiting cell proliferation (Fig. 2a, c). And SGC7901 cells with over-expressed PLIN2 gene contained a larger morphology and higher GFP brightness from the morphological point of view, indicating that the level of the target protein PLIN2 was elevated, which was confirmed by Rt-qPCR and Immunoblotting. Simultaneously, for MGC803, clonogenic assay showed that OvPLIN2 group contained more clones than Ovctrl, while the clonogenic rates of three SiRNA groups were lower than SiCtrl group (Fig. 2d, e). So the results of both over-expressed and knockdown groups are notably differential from the control group in SGC7901 and MGC803 cell lines.

Apoptotic capacity is depleted and ameliorated in MGC803, SGC7901 cell lines with elevation and elimination of PLIN2

The necrotic cells show red fluorescence after stained by Annexin V-PE, which can be used to forthrightly detect phosphatidylserine valgus as an essential feature of apoptosis by Flow Cytometry or fluorescence microscopy. In this experiment we discovered that the green MGC803

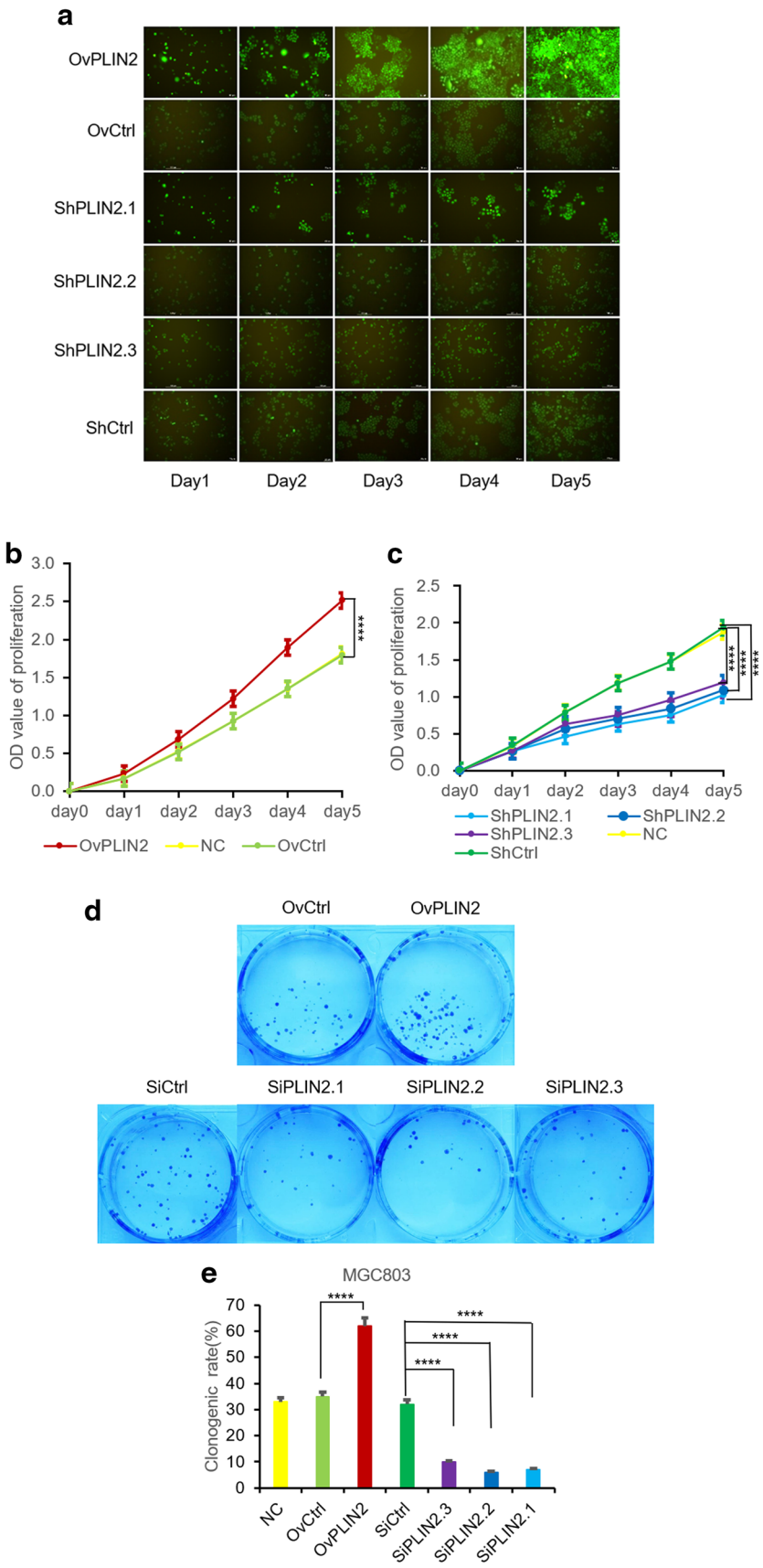

Fig. 2 Cell proliferation is accelerated and attenuated with enhancement and suppression of PLIN2. **a** Cell growth velocity was monitored among five groups by fluorescent microscope from day 1 to day 5, scale bar = 50um, the green indicated the stable transfected cells. The cells with OvPLIN2 were larger, higher convergence, more clonal colonies and brighter luminance than the control group. On the contrary, the cells with ShPLIN2 were smaller, scattered, fewer clones and darker luminance. **b** Higher proliferated capacity of SGC7901 with overexpression of PLIN2. **c** Decreasing proliferated capacity of SGC7901 with knockdown of ShPLIN2.1, 2,3. **d** Clonogenic assay for MGC803 among different groups. **e** OvPLIN2 group contained more clones than Ovctrl, the clonogenic rates of three SiRNA groups were lower than the SiCtrl group ****$P < 0.0001$

cells were animated cells, and the apoptotic cells were red color in the view of fluorescence microscopy (Fig. 3a). Only 6.04% apoptotic cells were assayed in OvPLIN2, but 69.62%, 62.87% and 45.12% apoptotic cells were explicitly observed in the three knockdown groups compared with SiCtrl (Fig. 3b, c). Annexin V-PE, labeled with red fluorescence, does not interfere with the green fluorescence of GFP that already expressed in cells. And PE can be stimulated by 495,545 or 564 nm excitation light and emit a peak of 575 nm fluorescence by flow cytometry, which identified that the apoptotic rate of OvPLIN2 was significantly lower than OvCtrl, and the apoptotic peak of OvCtrl remarkably shifted to the right (Fig. 3d). This study indicated the apoptotic rate in OvCtrl was 22.4%, while the apoptotic rate of OvPLIN2 was 8.63% for SGC7901 (Fig. 3e). Besides, the apoptotic rate of ShPLIN2.1, ShPLIN2.2 and ShPLIN2.3 was 81.63%, 74.8% and 48.73%, respectively, which was extremely higher than ShCtrl (Fig. 3f). The analogous tendency of the apoptosis between SGC7901 and MGC803 cells adequately interpreted that PLIN2 gene has an indispensable effect on apoptosis of gastric carcinoma cells, which affirmed that PLIN2 resisted cell apoptosis as an oncogene of gastric cancer.

Promotion and inhibition of PLIN2 affect survival capacity and ROS of gastric carcinoma cells

The survival rate of SGC7901 cells in OvPLIN2 was distinctively higher than OvCtrl (Fig. 3g), whereas the survival rates of ShPLIN2.1, ShPLIN2.2 and ShPLIN2.3 were exceedingly lower than ShCtrl (Fig. 3h). Meanwhile, the significant survival rates were displayed for MGC803 among OvPLIN2, OvCtrl, SiPLIN2.1, 2, 3 and SiCtrol groups (Fig. 3i, j). The detection of cell survival rate is also direct reflection of apoptosis, which is a traditional cell counting method to forthrightly observe the cellular survivance by microscopy. Therefore, this experiment intuitively manifested that PLIN2 gene prominently oppose the apoptosis of SGC7901 and MGC803 cells. Moreover, ROS value was less noticeable in the cells with OvPLIN2 than ShPLIN2 and SiPLIN2, indicating the germination of mitochondrial peroxidation stress response related to Ferroptosis (Fig. 3k, l). The results of all the above cell function experiments determined that PLIN2 play an important role in adjustment of biological functions for gastric cancer cells—SGC7901 and MGC803. When PLIN2 was over-expressed, it not only promoted cell proliferation but also decelerated cell apoptosis, while when PLIN2 is lower-expressed, it suppressed cell proliferation but facilitated cell apoptosis. To identify no influence of transfected vectors on all the functional experiments, we also inspected the cell structure and function of NC group, which were not starkly discrepant from the two control groups. It is more principal to knock down PLIN2 to confirm that it is a typical oncogene of gastric cancer, because only knockdown can incarnate the veritable function for studying up-regulating gene and protein. In our study, three inferiorly expressed PLIN2 groups reflected remarkable elimination effects of PLIN2 on cellular proliferation, apoptosis and survival, respectively.

Tumoricidal reflection of PLIN2 variation in vivo

Tumorigenesis occurred within 1 week after subcutaneous injection. The neoplastic growth velocity in the mice injected into SGC7901 cells with OvPLIN2 was notably faster since the seventh day, which was apparently higher than the mice injected into the cells with Control. Meanwhile, the tumor of ShPLIN2 group grew extremely more dilatory than Control group since the 12th day (Figs. 4a, b and s1). The results were sufficient to corroborate that the modulation of PLIN2 on proliferation and apoptosis in vitro had been completely confirmed in vivo. Furthermore, the mice in OvPLIN2 group displayed the ultimate body weight and size, but those in ShPLIN2 group exhibited the minimal body weight and size, suggesting that PLIN2 contributed to the growth of tumors caused by abnormal lipid metabolism (Fig. 4c, e). The expressed differences of PLIN2 level among three groups were validated by Rt-qPCR (Fig. 6a), Immunoblotting (Fig. 6b, c) and IHC (Fig. 6d), respectively. HE staining demonstrated the increasing of necrotic areas due to excessive cell proliferation in OvPLIN2 group compared to the other two groups (Fig. 4d).

PLIN2 modulates the differentially expressed genes among OvPLIN2, Control, ShPLIN2 xenografts

Three groups of mice tumors were analyzed for RNA-seq detection. Firstly, according to the gene expression level of each sample, 120 up-regulated genes and 1018 down-regulated genes of total 1138 differentially expressed genes (DEGs) were examined between Control and OvPLIN2 (Fig. 5a). And 282 high-expressed genes and 345 low-expressed genes of total 627 DEGs were detected between Control and ShPLIN2 (Fig. 5b). Moreover, the expression of 1184 genes were raised and 332 genes were descended in total 1516 DEGs between ShPLIN2 and OvPLIN2 (Fig. 5c). The screening conditions were log2-fold change (log2FC) ≥ 2 and $P \leq 0.001$. Then we applied Venn diagram to display the situation of genes in distinct comparative groups for DEG data in multiple comparative groups, containing 86 common DGEs in Control VS OvPLIN2, Control VS ShPLIN2 and ShPLIN2 VS OvPLIN2 (log2FC ≥ 2 and $P \leq 0.001$) (Fig. 5d). In addition, we continued to establish cluster analysis with screening condition of level FPKM ≥ 10 (Fragments Per Kilobase of transcript per Million fragments mapped), and the difference-multiple log2FC ≥ 2

and $P \leq 0.001$ (Fig. 5e). And Cluster thermogram palpably described the difference of gene expression with PLIN2 variation in three groups. The various color blocks were selected for cluster analysis. The red represented an obviously high-expressed genes and the blue represented apparently low-expressed genes. The purpose of combining above two methods was to reduce the scope of screening differentially expressed genes. Furthermore, GO Functional Enrichment Analysis presented that the enriched genes that affected by PLIN2 mainly participated in the Lipid-metabolic process (Fig. 5f). And KEGG pathway analysis described that Ferroptosis pathway was cardinal one of the twenty pathways involved in differentially expressed genes among the selected groups (Fig. 5g).

PLIN2 regulates the mechanism of Ferroptosis pathway included the genes and proteins ACSL3, ALOX15, LC3A, PRDM11, IPO7

The Ferroptosis pathway contained genes ACSL3, ALOX15, LC3A, PRDM11, IPO7 which were markedly differentially expressed among the three groups. This affirmed that these genes are potentially modified by PLIN2: when PLIN2 was overexpressing, the expression of ACSL3, ALOX15, LC3A, PRDM11 decreased in Ferroptosis pathway, while the expression of IPO7 increased. When PLIN2 was knocked down, the expression of ACSL3, ALOX15, LC3A, PRDM11 improved and the expression of IPO7 descended. The results had been verified by Rt-qPCR (Fig. 6a) Immunoblotting (Fig. 6b, c) and IHC (Fig. 6d, e), respectively. In Rt-qPCR verification, the hybrid DNA in the extracted total RNA had been removed before reverse transcription, to avert the interference and ensure the accuracy of the PCR results. Immunohistochemical results revealed that the expression of target protein PLIN2 in OvPLIN2 was intensely positive, while that was undoubtedly attenuated in ShPLIN2. Above all proteins that expressed discrepantly in tissues by the modulation of PLIN2, which was consistent with the results of Rt-qPCR, Immunoblotting and IHC. Besides, we also depicted protein–protein interaction (PPI) to make predictive analysis to definitely visualized the interaction between PLIN2 and the proteins ACSL3, ALOX15, LC3A, PRDM11, IPO7 included in the Ferroptosis pathway. The red was the up-regulated protein modified by PLIN2, and the blue was the downregulated protein dominated by PLIN2 (Fig. 6f).

PLIN2 modifies lipid metabolism of gastric cancer

The size and number of intracellular lipid droplets of each group were observed by Nile Red Fluorescence staining (Fig. 7a, c). The fluorescence intensity showed that lipid droplets in cells with over-expressing PLIN2 were larger and more, while those in cells with low-expressing PLIN2 were smaller and fewer (Fig. 7b, d). Additionally, micro-assay was performed on mice tumor tissues to verify the higher fat mass in OvPLIN2 than in ShPLIN2 according to the content of triglycerides (Fig. 7e). And the body size of mice was measured and evaluated by Lee's Index. The results showed that there was no significant difference in the length of mice among the groups, indicating that the variation of body weight was affected by PLIN2 level (Fig. 7f).

Fig. 3 Apoptotic capacity is depleted and ameliorated in MGC803, SGC7901 cell lines with elevation and elimination of PLIN2, Promotion and inhibition of PLIN2 affect survival capacity and ROS of gastric carcinoma cells. **a** Detection of apoptotic MGC803 cells without FBS for 48 h by fluorescent microscope, the red and the green represented apoptotic and viable cells, respectively, scale bar 100 μm. **b**, **c** For MGC803 cells, the apoptotic rate of over-expressed PLIN2 group was lower than OvCtrl, while that of low-expressed PLIN2 groups SiPLIN2.1, SiPLIN2.2 and SiPLIN2.3 were significantly higher than SiCtrl. **d** Flowcyto assay showed apoptotic peaks on the right side by Annexin V-PE staining. **e**, **f** For SGC7901, the apoptotic percentage was, respectively, reduced and elevated with up and downregulated PLIN2. **g**, **h** Survival rate of SGC7901 among different groups. **i**, **j** Survival rate of MGC803 among different groups. **k** ROS values among all groups for SGC7901. **l** ROS values among all groups for MGC803. $^{**}P < 0.01$; $^{***}P < 0.001$; $^{****}P < 0.0001$

Discussion

An increasing number of tumors are associated with abnormal lipometabolism, such as gastric cancer, intestinal cancer, renal cancer, esophageal cancer, pancreatic cancer, and so on, but the specific mechanism is still uncertain. PLIN2, a protein encoded by PLIN2 gene, which promotes cell adipose differentiation and provides energy for cell growth [11]. PLIN2 is unexpectedly expressed in some neoplastic tissues and cells, such as renal clear-cell carcinoma [12], but few research focus on stomach neoplasm, and the mechanism of PLIN2 gene involved in the occurrence and development of gastric cancer is indistinct. In our study, PLIN2 provided energy for the proliferation of gastric carcinoma cells and retardation of the apoptosis. We discovered that the cell morphology transformed conspicuously and the cellular shape became larger during the process of cell culture after PLIN2 gene was successfully and stably transfected into SGC7901 cell line, which were conductive to raise the contiguous area and confluent capacity among the cells. So the cells proliferated faster, and steadily overexpressing PLIN2 transfection-period was 2 months, while ShRNA transfection into SGC7901 cells consumed 3 months due to the tardy growth of cells after PLIN2 gene was knockdown without lucid variation in cell morphology compared with NC. The instantaneous transfection of SiRNA was performed into MGC803 cell line to knockdown PLIN2 owing to the

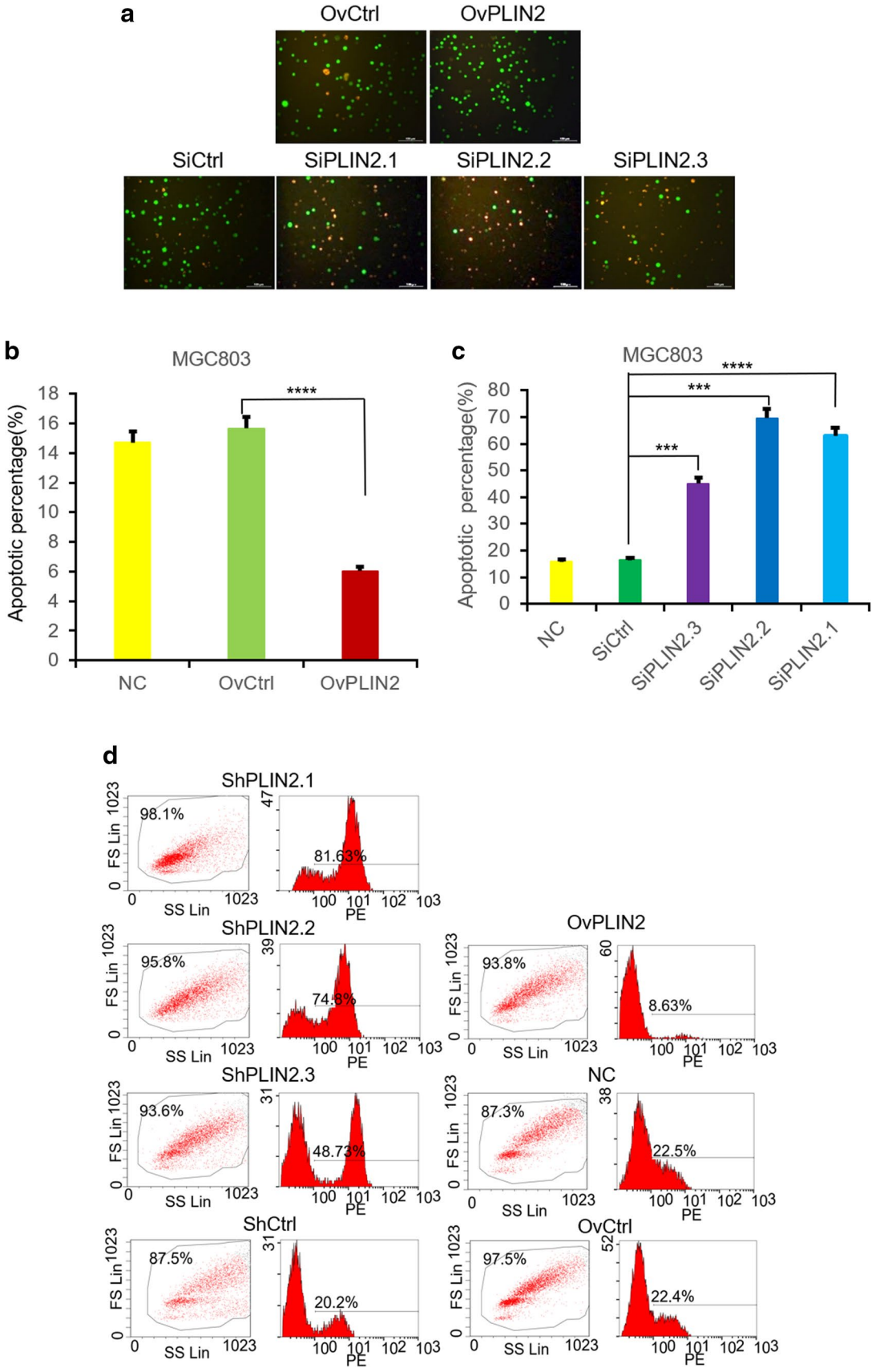
a
OvCtrl
OvPLIN2
SiCtrl
SiPLIN2.1
SiPLIN2.2
SiPLIN2.3
b
MGC803
Apoptotic percentage(%)
****
NC
OvCtrl
OvPLIN2
c
MGC803
Apoptotic percentage(%)
****
***
***
NC
SiCtrl
SiPLIN2.3
SiPLIN2.2
SiPLIN2.1
d
ShPLIN2.1
98.1%
81.63%
ShPLIN2.2
95.8%
74.9%
OvPLIN2
93.8%
8.63%
ShPLIN2.3
93.6%
48.73%
NC
87.3%
22.5%
ShCtrl
87.5%
20.2%
OvCtrl
97.5%
22.4%
FS Lin
SS Lin
PE

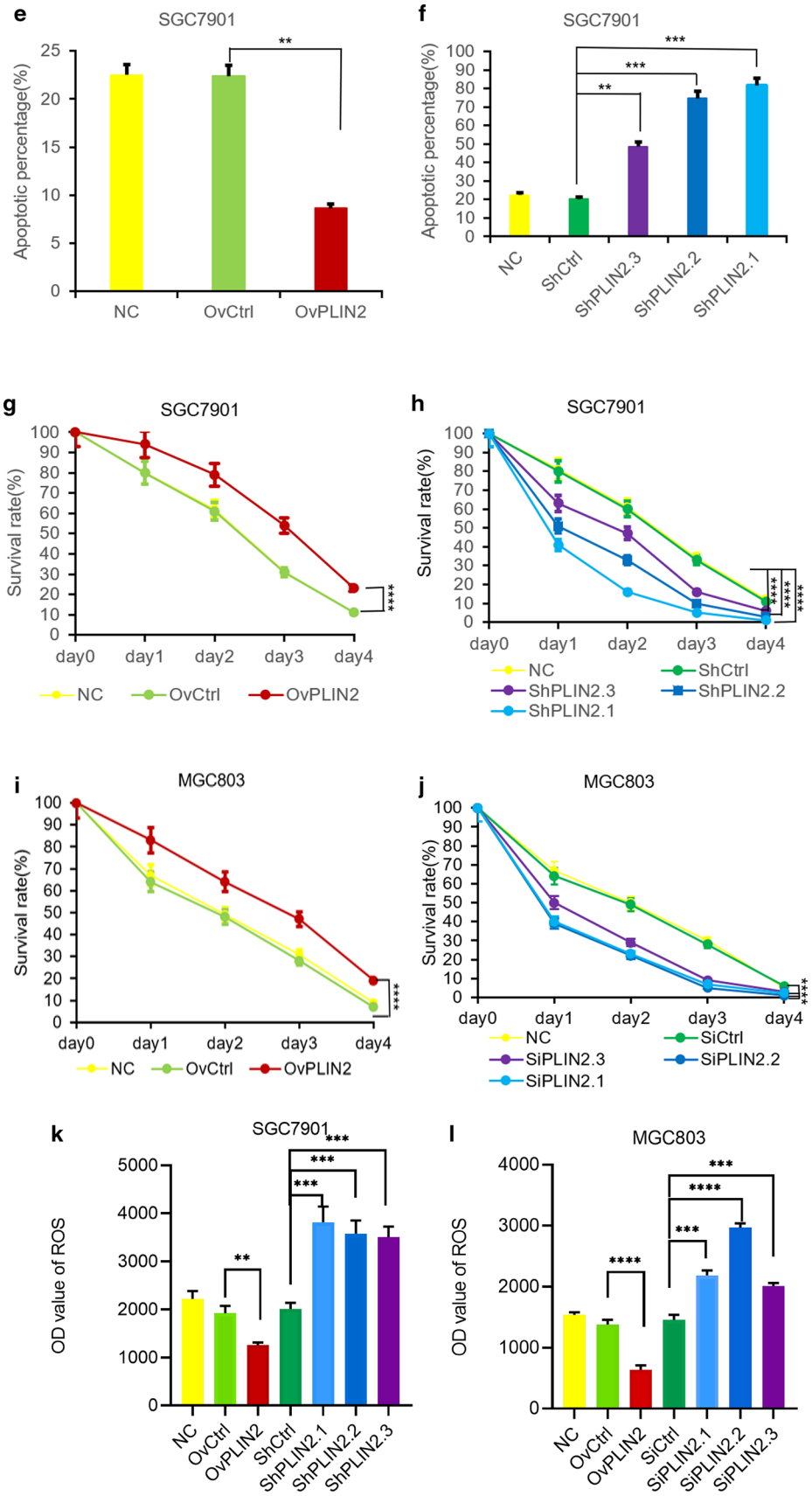

Fig. 3 (continued)

larger cell morphology, more vulnerable transfection and the higher transfected efficiency. Meanwhile, the survival rate of PLIN2 over-expressed cells was strikingly superior but was inferior in ShPLIN2 groups. Furthermore, the proliferation and viability of PLIN2 over-expressed cells or ShPLIN2 downexpressed cells elevated or reduced remarkably. Consequently, it was manifested that PLIN2 obtains a prominent effect on promoting the proliferation and suppressing the apoptosis of gastric cancer cells.

The principal point in vivo is that PLIN2 was involved in the gene regulation of Ferroptosis pathway and lipid metabolism. Ferroptosis is a novel type of programmed cell death that was found recently with few studies on stomach neoplasm at present. Ferroptosis conduces to cell death dependent on iron and characterized by the accumulation of lipid peroxides [13]. In our study, overexpression and knockdown of PLIN2 can decrease and increase the intracellular ROS content. Our explanation is that the occurrence of oxidative stress requires more oxygen, but the high lipid content, that is, overexpressed PLIN2, can lead to relative hypoxia in cells, thus inhibiting Ferroptosis and promoting neoplastic formation. It has been reported that PLIN2 is overexpressed in ccRCC and positively correlated with hypoxia inducible factor—HIF2alpha activation [12], which is consistent with our explanation. Besides, Flow Cytometry and fluorescent microscopy were, respectively, applied to corroborate that the apoptotic tendency of SGC7901 and MGC803 was unanimous when PLIN2 was knocked down by different transfection methods. Regardless of SGC7901 and MGC803, the morphological variation of Ferroptosis such as cell shrinkage and apoptotic bodies could be observed within 48 h after induction of apoptosis, while the morphological transformations of PLIN2 over-expressed cells were trivial, but the apoptotic property of ShPLIN2 or SiRNA cells were more evident than the control. Ferroptosis is initiated by the failure of the glutathione-dependent antioxidant defenses, resulting in unchecked lipid peroxidation and eventual cell death [14]. Lipophilic antioxidants, and iron chelators can prevent ferroptotic cell death [15]. In our study, OvPLIN2 and ShPLIN2 were displayed predominant differences with expression of genes involved in ferroptotic process by RNA-seq. The negatively regulatory genes involved ACSL3, ALOX15, LC3A, PRDM11, and the positively regulatory gene was IPO7. The protein encoded by ACSL3 gene belongs to an isozyme of the long-chain fatty-acid-coenzyme A ligase family. Studies have reported that ACSL4 is one of the essential components of iron death by participating in the synthesis of these oxidizable membrane phospholipids, and it can be used as an indicator of whether cells can initiate iron death [16]. As an isoenzyme of ACSL4, so far the diverse standpoints on the expression of ACSL3 in tumors still exist, such as the higher expression of ACSL3 in prostate cancer cells [17]. Whereas, other researchers declared

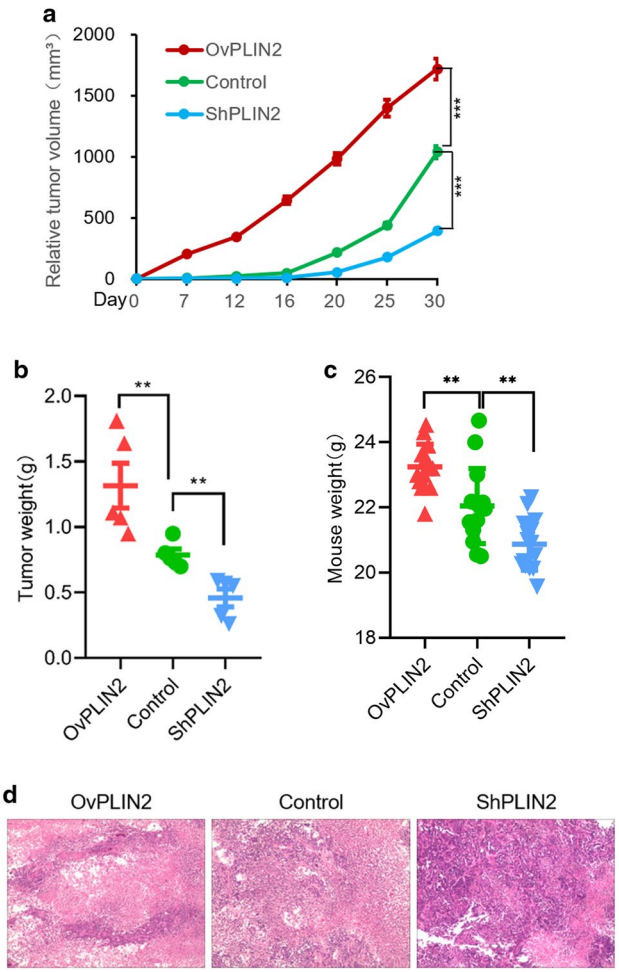

Fig. 4 Tumoricidal reflection of PLIN2 variation in vivo. **a** Tumor growth curve of subcutaneous OvPLIN2, control, ShPLIN2 xenografts in nude mice within 30 days, the relative tumor volume (RTV) was calculated and compared every 4 days. **b** Weight of OvPLIN2, Control, ShPLIN2 tumors as indicated, Mean tumor weight ± SEM are shown in 5 mice per group. **c** Weight of OvPLIN2, Control, ShPLIN2 mice as indicated. **d** HE staining showed the distinctive proliferation and necrosis among tissues of three groups, 4 × 10 fold. $^{*}P < 0.05$; $^{**}P < 0.01$; $^{***}P < 0.001$

that among the five family isoforms, ACSL1 and ACSL4 are able to promote ungoverned cell growth, facilitate tumor invasion and evade programmed cell death, while ACSL3 may have relatively complex functions in various types of cancer [2]. In our study, ACSL3 hastened the apoptosis of gastric cancer cells by blocking the expression of PLIN2, thus restraining the proliferation of cancer cells. So the expression of ACSL3 decreased when PLIN2 gene was overexpressing. Hence, it was a restrainer in gastric cancer tissues confirmed by Rt-qPCR, Immunoblotting and IHC. What's more, our RNA-seq analysis indicated that the ACSL family also participate in essential lipid metabolism pathways, such as Peroxisome Adipocytokine signaling pathway, Fatty acid metabolism including biosynthesis and

degradation PPAR signaling pathway, which revealed that ACSL family is a vital determinant of lipid metabolism. Moreover, ALOX15, like other lipoxygenases, a seminal enzyme in the metabolism of polyunsaturated fatty acids to a wide range of physiologically and pathologically central products. Kalamkari and Badr announced that the ALOX15 gene product is implicated in antiinflammation, membrane remodeling, and cancer development and metastasis [18]. Numerous researches have alleged that ALOX15 expression is downregulated in colorectal cancer as an antioncogene [19]. It might be a trigger that a declined 15-LOX-1 expression in the endometrial tumorigenesis process, can induce starting from normal endometrium to hyperplasia and endometrial cancer [20]. Likewise, our study illustrated that the ascent of PLIN2 expression contribute to a descending ALOX15 expression, arrest the occurrence of Ferroptosis and prevent cells from apoptosis. Conversely, knockdown of PLIN2 facilitated ALOX15 higher expression and acceleration of Ferroptosis. Thus, it was concluded that ALOX15 is governed by PLIN2 as a gastric cancer retardant. In this study, we also explored that ALOX15 not only participated in the Ferroptosis pathway, but also in Necroptosis, Arachidonic acid metabolism and Linoleic acid metabolism, which demonstrates that ALOX15 was involved in the regulation of cell lipid metabolism and apoptotic necrosis by the modification of PLIN2. And IHC also explicated that gastric neoplastic cells are accompanied by diverse degrees of inflammation, neoplastic cells coexisted with inflammatory cells. Besides, ALOX15 was intensely expressed in inflammatory cells with anti-inflammatory capacity, but weakly expressed in neoplastic cells. As consequence, anti-inflammatory reaction may accelerate apoptosis of neoplastic cells. Because PLIN2 knockdown tissues comprised majority of inflammatory cells and few tumor cells, the intense expression of ALOX15 could initiate the regression of inflammation and repress the growth of tumor cells. Thus, we authenticated ALOX15 played a puissant role in the balance between inflammation and cancer. In addition, LC3A is an indispensible gene involved in autophagy, which is the natural, regulated mechanism of the cell that disassembles unnecessary or dysfunctional components. It allows the orderly degradation and recycling of cellular components [21]. Studies have proved that LC3A is essential for autophagy and impairment of autophagy induces DNA damage leading to genetic instability and carcinogenesis [22]. Likewise, our study detected that PLIN2 negatively adjust LC3A, because the expression of LC3A elevated with PLIN2 decreasing, which concurrently accelerated the occurrence of autophagy, apoptosis and necrosis of gastric cancer cells. And we also demonstrated the contrary outcome if PLIN2 expression heightened. Furthermore, PRDM11 gene is composed of one PRDF1-RIZ (PR) homology domain as the only member of PRDM family without zinc-finger structure, its potential methyltransferase activity is followed by a variable number of zinc-finger motifs, which likely mediate protein–protein, protein–RNA, or protein–DNA interactions, PRDM family plays a decisive role in cell differentiation, proliferation and disease regulation with affecting epigenetics [23]. The PR-domain (PRDM) family of genes encodes transcriptional regulators, several of which are deregulated in cancer, overexpression of PRDM11 inhibits proliferation and induces apoptosis [24]. However, PRDM11 has not been studied in gastric cancer at present, in our study, PRDM11 was negatively regulated by PLIN2 protein and became a retardant of gastric cancer with obstruction in the proliferation of gastric cancer cells and benefiting cell apoptosis. Accordingly, PRDM11 was probably a novel gastric cancer restrainer as transcription factor. So to explore its molecular mechanism contributes to study the epigenetic regulation of cell proliferation and differentiation in gastric cancer. Additionally, Importin 7 (IPO7) was the only gene positively altered by PLIN2 in Ferroptosis pathway in our study. It is a relatively conserved class of proteins widely distributed in eukaryotes that transport transcription factors, splicing factors and other proteins in the cytoplasm to the nucleus through nuclear pore complexes. At present, no studies on IPO7 in gastric cancer have been found. As another novel gene, IPO7 is considered a non-redundant component of an intrinsic pathway in mammalian cells for efficient accumulation of exogenous and endogenous DNA in the nucleus, which presumably be critical for the exchange of genetic information between mitochondria and nuclear genomes [25]. And one

Fig. 5 PLIN2 modulates the differentially expressed genes among OvPLIN2, Control, ShPLIN2 xenografts. **a**–**c** DEGs among three comparative groups were displayed by volcanic maps. The *X*-axis represents the difference multiples after log2 conversion, and the *Y*-axis represents the significant value after log10 conversion. The red one represents up-regulated DEGs, The blue one represents down-regulated DEGs, and the gray one represents non-DEG. log2FC ≥ 2 and $P < 0.001$. **d** Venn diagram described DGEs in control VS OvPLIN2, control VS ShPLIN2 and ShPLIN2 VS OvPLIN2. log2FC ≥ 2 and $P \leq 0.001$. **e** Cluster analysis was conducted on the FPKM value of each comparative group.17 genes were related to PLIN2. Thermogram illustrated that log2 (FPKM + 1) of the sample was represented by the horizontal axis and the gene was represented by the vertical axis. Under default color matching, the redder the color of the block, the higher the expression level, the bluer the color, the lower the expression level. **f**, **g** Bubble diagram showed GO functional enrichment and KEGG pathway enrichment analysis. *X*-axis is enrichment ratio [the ratio of the number of genes annotated to an item in a selected gene concentration to the total number of genes annotated to that item in the species, the formula is Rich Ratio = Term Candidate Gene Num/Term Gene Num], *Y*-axis is GO Term or KEGG Pathway, the size of bubbles represents the number of genes annotated to a GO Term or KEGG Pathway, the color represents enrichment *Q* value, and the darker the color represents *Q* value, the smaller the value. *Q* value is the calibration value of *P* value

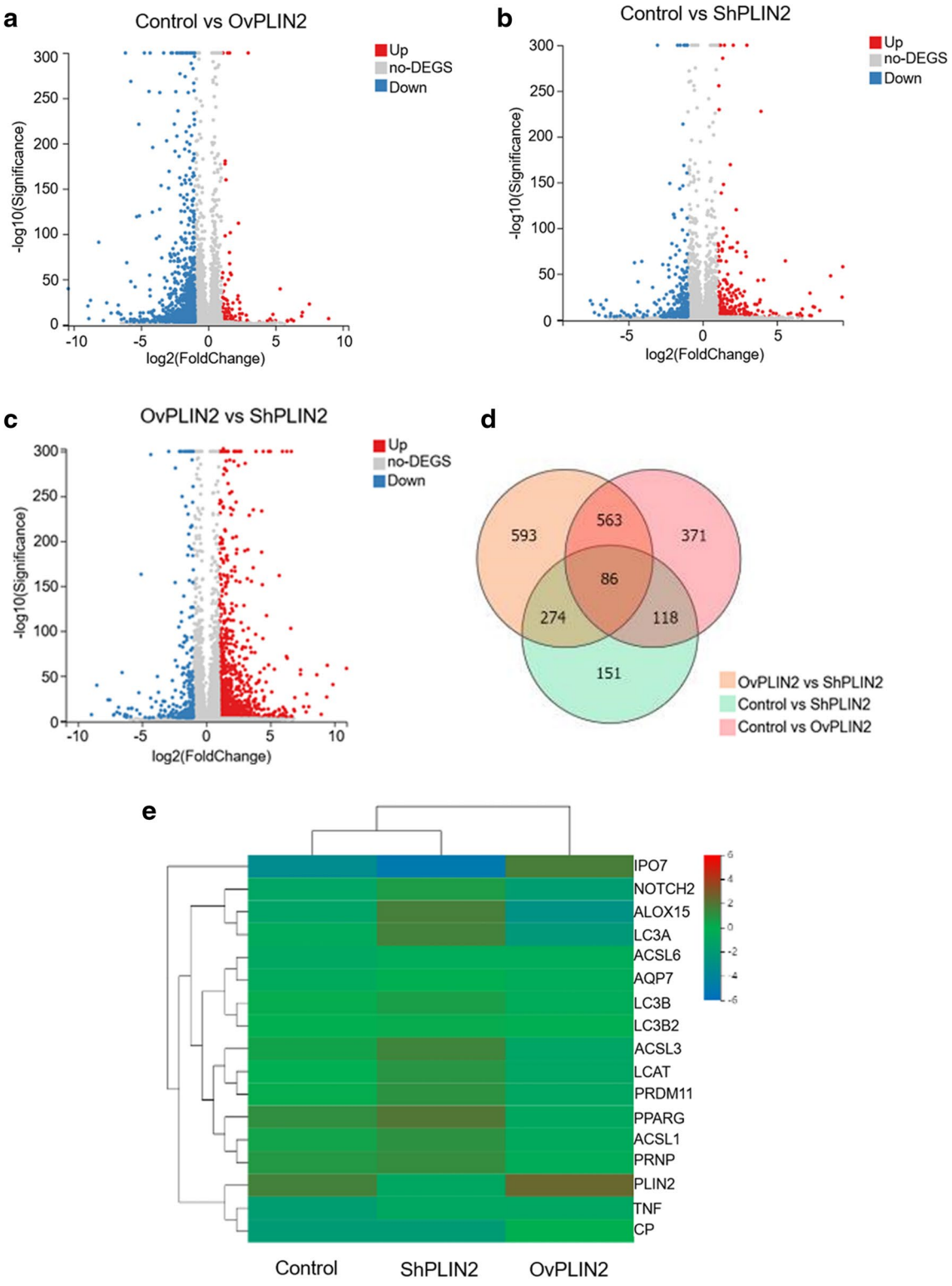
a
Control vs OvPLIN2
Up
no-DEGS
Down
-log10(Significance)
log2(FoldChange)
b
Control vs ShPLIN2
Up
no-DEGS
Down
-log10(Significance)
log2(FoldChange)
c
OvPLIN2 vs ShPLIN2
Up
no-DEGS
Down
-log10(Significance)
log2(FoldChange)
d
593
563
371
86
274
118
151
OvPLIN2 vs ShPLIN2
Control vs ShPLIN2
Control vs OvPLIN2
e
IPO7
NOTCH2
ALOX15
LC3A
ACSL6
AQP7
LC3B
LC3B2
ACSL3
LCAT
PRDM11
PPARG
ACSL1
PRNP
PLIN2
TNF
CP
Control
ShPLIN2
OvPLIN2

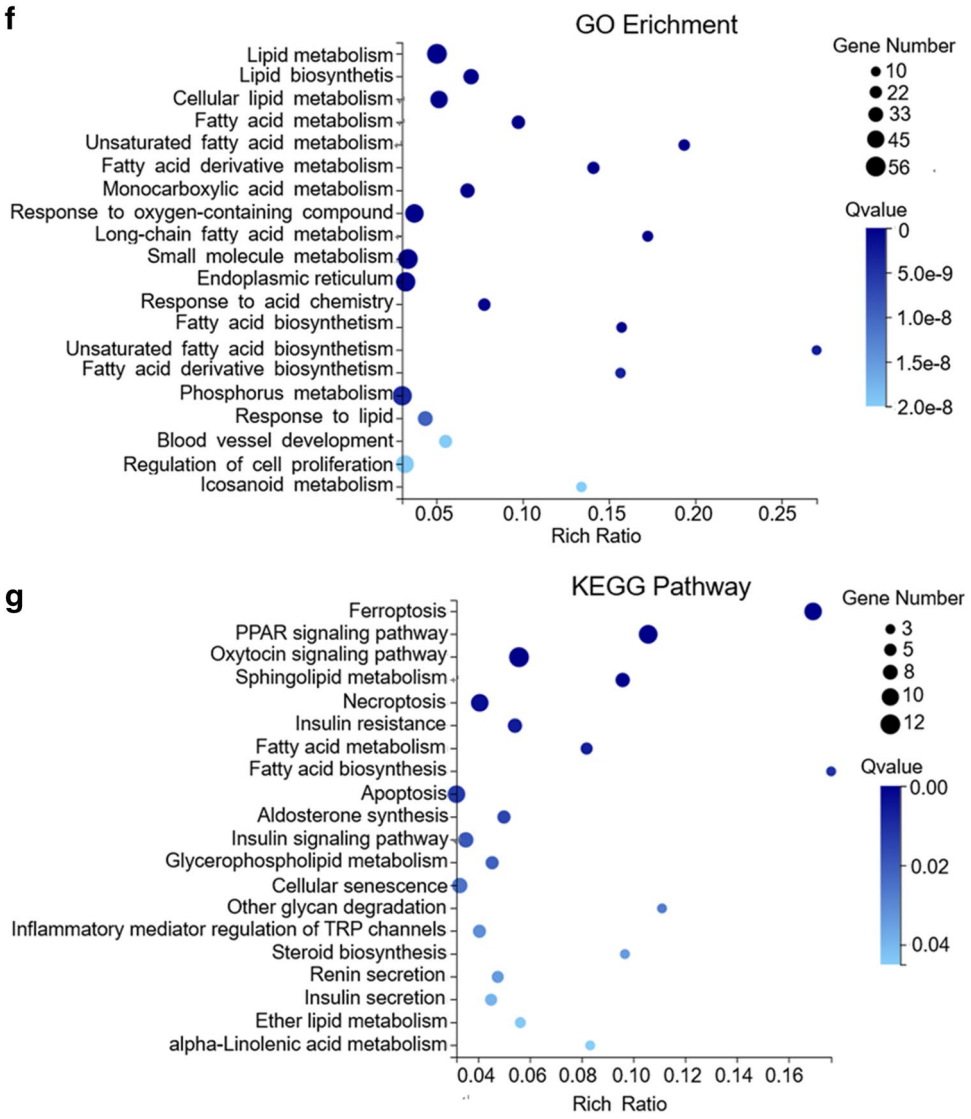

Fig. 5 (continued)

researcher discussed activation of the innate immune response made IPO7 level elevated in Aspc-1 and Hs700T pancreatic cancer cells [26]. Similarly, our study suggested that PLIN2 expression increasing cause IPO7 enhancement with the amelioration of cell proliferation as a new transcription factor for gastric cancer cells.

In conclusion, the occurrence and development of any cancer are related to proliferation and apoptosis. Only inhibiting the proliferation and promoting the apoptosis of cancer cells may facilitate the neoplastic treatment. In this study, we discovered that PLIN2 modulated Ferroptosis pathway through regulating transcription factors-PRDM11 and IPO7:ACSL3 was a critical gene involved in abnormal lipid metabolism, ALOX15 facilitated apoptosis and necrosis. LC3A promoted autophagy and PRDM11 suppressed gastric cancer. Above all genes can be downregulated by PLIN2 during Ferroptosis process; IPO7 level was elevated after the stimulation of PLIN2, and it provided energy for cell proliferation and resisted Ferroptosis as gastric oncogene and cell-importing protein. Ferroptosis is implicated in complex biochemical reactions, gene expression and signal transduction, and has become prevalent in the

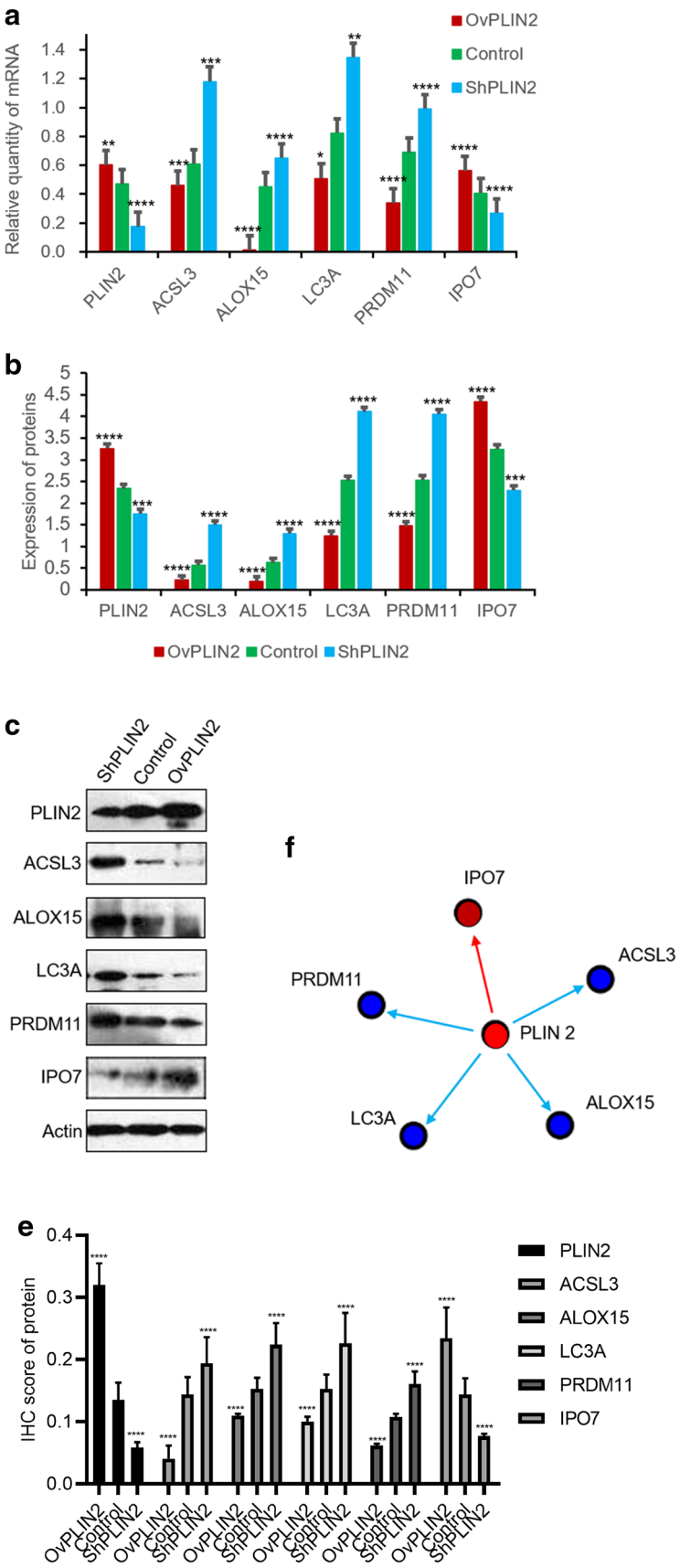

Fig. 6 PLIN2 regulates the mechanism of Ferroptosis pathway and lipid metabolism included the genes and proteins ACSL3, ALOX15, LC3A, PRDM11, IPO7. **a** Level of tumor mRNA for PLIN2, ACSL3, ALOX15, LC3A, PRDM11, IPO7 among OvPLIN2, Control, ShPLIN2 groups. **b** Expression of tumor proteins PLIN2, ACSL3, ALOX15, LC3A, PRDM11, IPO7 in OvPLIN2, Control, ShPLIN2 tumors. **c** Immunoblotting for the expression of specific proteins regulated by PLIN2, Actin was loading control. **d**, **e** IHC showed six differently expressed proteins among mice tumors of three groups, NC was staining control. **f** For PPI, the red represented up-modulated IPO7 by PLIN2, the blue represented downregulated ACSL3, ALOX15, LC3A, PRDM11 by PLIN2. $*P<0.05$; $**P<0.01$; $***P<0.001$; $****P<0.0001$

Fig. 6 (continued)

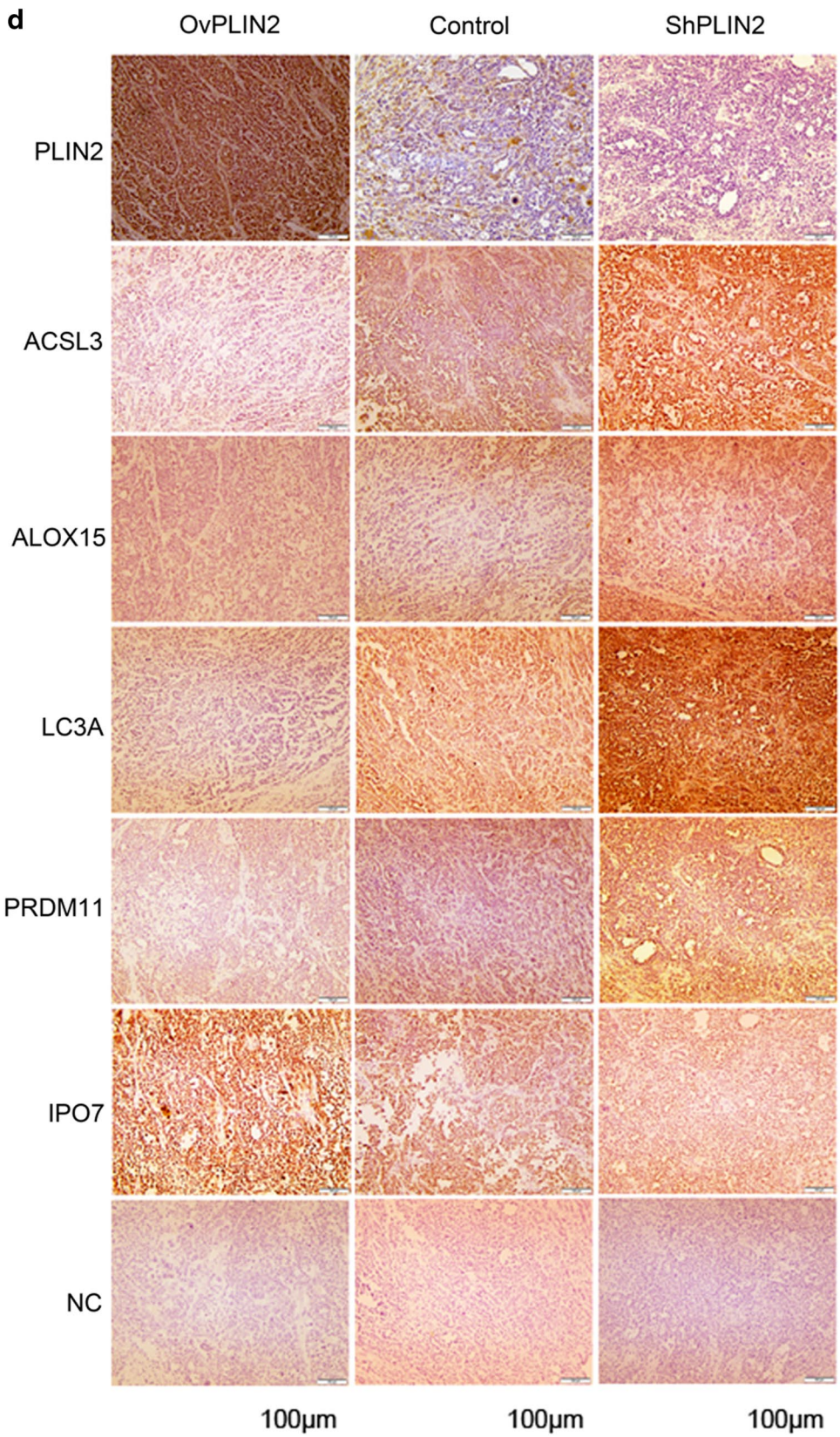

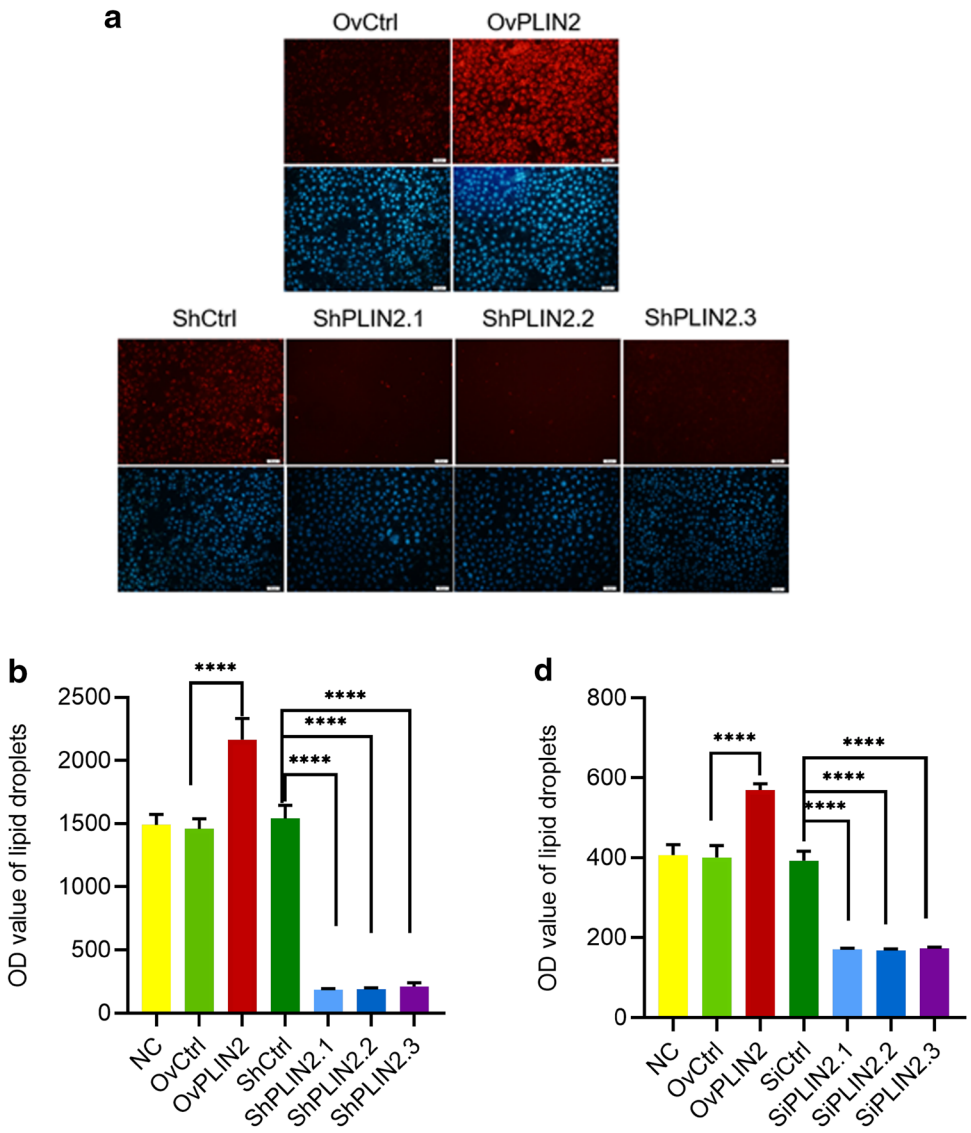

Fig. 7 High or low level of PLIN2 induces excessive or minor lipid content of gastric cancer in vitro and vivo. **a** Nile Red Fluorescence staining showed the intracellular lipid droplets in SGC7901, the red is Nile Red, the blue is Hoechst Fluorescence for cell nucleus staining, scale bar 50 μm. **b** OD value of lipid droplets were detected at 552/636 nm for SGC7901. **c** Nile Red Fluorescence staining showed the intracellular lipid droplets in MGC803, the red is Nile Red, the blue is Hoechst Fluorescence, for cell nucleus staining, scale bar = 50 μm **d** OD value of lipid droplets were detected at 552/636 nm for MGC803. **e** OD value of triglyceride in mouse tumors were evaluated by microassay at 420 nm. **f** Lee's index for evaluation of mouse body size. $^{*}P < 0.05$; $^{****}P < 0.0001$

international research recently. Our study stated that PLIN2 inhibited Ferroptosis and facilitated the advancement of gastric carcinoma, which sufficiently expounded the importance of PLIN2 gene and protein in the occurrence and the mechanism of obesity leading to the formation of gastric neoplasm. Simultaneously, two novel genes PRDM11 and IPO7 were explored in the Ferroptosis pathway, which perhaps be involved in the transcriptional regulation of genes related to gastric carcinoma. Nevertheless, it is still indeterminate whether PLIN2 is involved in other pathways or transcription factors related to the metabolism of gastric carcinoma, so further investigations are required. Therefore, PLIN2 probably be applied as a potential biomarker for gastric neoplastic diagnosis and therapeutic target, especially for the prediction of tumors from obese patients in the future.

Fig. 7 (continued)

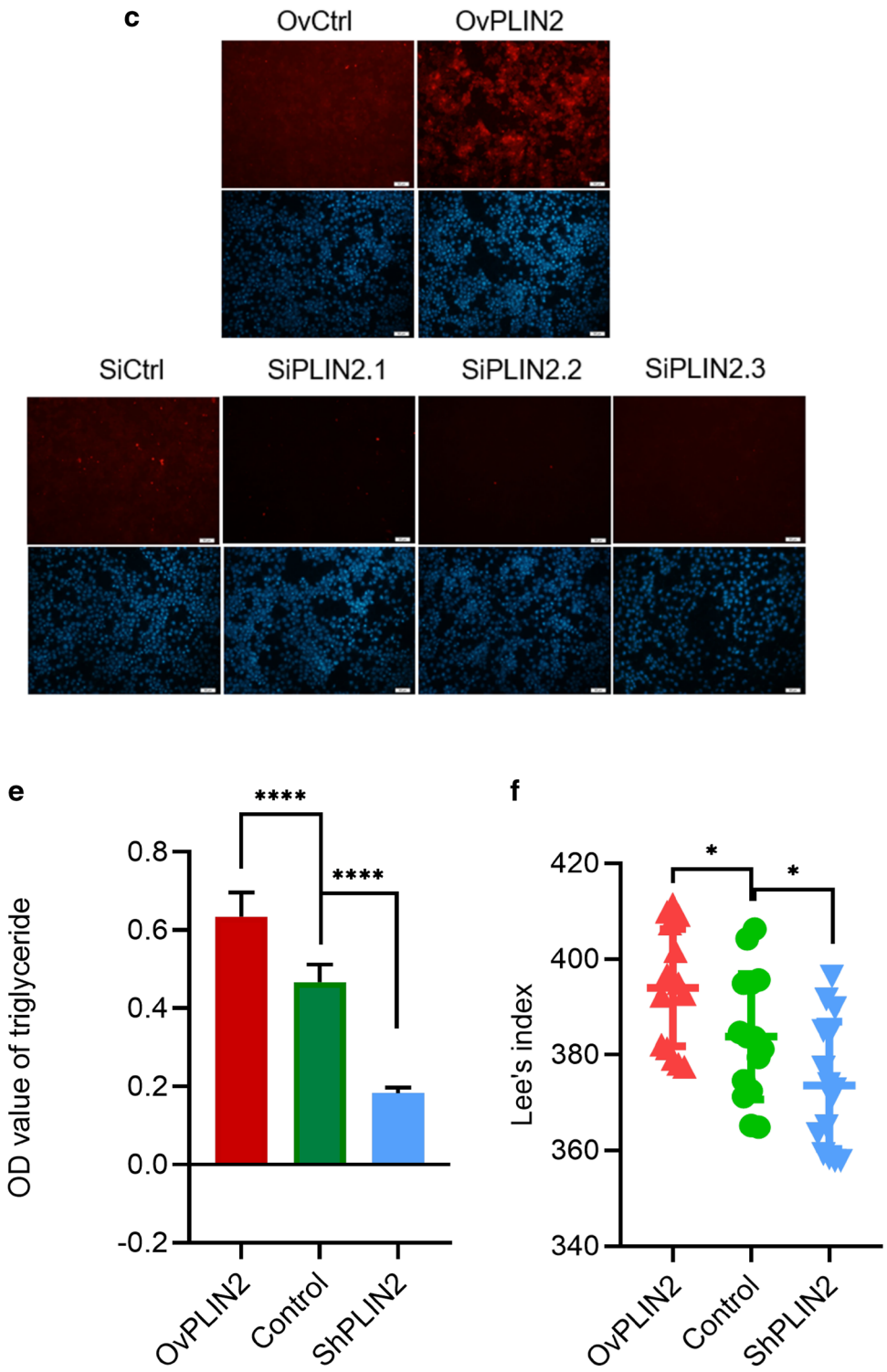

Statistical analysis

T test or one-way ANOVA with Bonferroni post-test was properly applied to calculate and analyze statistical significance with GraphPad Prism 8.0 software. A *P* value less than 0.05 was considered statistically significant.

Acknowledgements We would like to express our gratitude to Tissue Bank and Department of Science Research Center of China-Japan Union Hospital of Jilin University.

Author contributions CYH and YWZ designed the experiments. XYS, SJY, XCF performed the experiments, XYS wrote the manuscript.

HW, JSZ, HYS and YCZ checked the manuscript. All authors read and approved the final manuscript.

Funding The study was supported by National Natural Science Foundation of China (81572082), Science and Technology Development Project of Jilin Province (20140311092YY), and Jilin Provincial Science and Technology Agency Project (2011713, 20150414015GH and 20150101153JC), Industrial Technology Research and Development (2019CO49-6).

Compliance with ethical standards

Conflict of interest The authors declare no conflicts of interest.

Ethics standards The animal studies were implemented in accordance with the stipulations of Laboratory Animal Welfare Ethics Committee at Jilin University (Certificate of Approval NO. pzpx201809290244). All institutional and national guidelines for the care and use of laboratory animals were followed.

Human rights statement and informed consent All procedures followed were in accordance with the ethical standards of the responsible committee on human experimentation (institutional and national) and with the Helsinki Declaration of 1964 and later versions. Informed consent to be included in the study, or the equivalent, was obtained from all patients.

References

1. Wu D, Zhang P, Ma J, Xu J, Yang L, Xu W, et al. Serum biomarker panels for the diagnosis of gastric cancer. Cancer Med. 2019;8:1576–83 **(Epub ahead of print)**.
2. Tang Y, Zhou J, Hooi SC, Jiang YM, Lu GD. Fatty acid activation in carcinogenesis and cancer development: essential roles of long-chain acyl-CoA synthetases. Oncol Lett. 2018;16:1390–6.
3. Ueo T, Yonemasu H, Yada N, Yano S, Ishida T, Urabe M, et al. White opaque substance represents an intracytoplasmic accumulation of lipid droplets: immunohistochemical and immunoelectron microscopic investigation of 26 cases. Dig Endosc. 2013;25:147–55.
4. Orlicky DJ, Degala G, Greenwood C, Bales ES, Russell TD, McManaman JL. Multiple functions encoded by the N-terminal PAT domain of adipophilin. J Cell Sci. 2008;121:2921–9.
5. Conte M, Franceschi C, Sandri M, Salvioli S. Perilipin 2 and age-related metabolic diseases: a new perspective. Trends Endocrinol Metab. 2016;27:893–903.
6. Gushima R, Yao T, Kurisaki-Arakawa A, Hara K, Hayashi T, Fukumura Y, et al. Expression of adipophilin in gastric epithelial neoplasia is associated with intestinal differentiation and discriminates between adenoma and adenocarcinoma. Virchows Arch. 2016;468:169–77.
7. Hassannia B, Vandenabeele P, Vanden Berghe T. Targeting Ferroptosis to iron out cancer. Cancer Cell. 2019;35(6):830–849. https://doi.org/10.1016/j.ccell.2019.04.002.
8. Friedmann Angeli JP, Krysko DV, Conrad M. Ferroptosis at the crossroads of cancer-acquired drug resistance and immune evasion. Nat Rev Cancer. 2019;19(7):405–414. https://doi.org/10.1038/s41568-019-0149-1.
9. Masaldan S, Bush AI, Devos D, Rolland AS, Moreau C. Striking while the iron is hot: Iron metabolism and ferroptosis in neurodegeneration. Free Radic Biol Med. 2019;133:221–33.
10. Yamaguchi Y, Kasukabe T, Kumakura S. Piperlongumine rapidly induces the death of human pancreatic cancer cells mainly through the induction of ferroptosis. Int J Oncol. 2018;52(3):1011–22. https://doi.org/10.3892/ijo.2018.4259. **(Epub 2018 Jan 31)**.
11. Sztalryd C, Kimmel AR. Perilipins: lipid droplet coat proteins adapted for tissue-specific energy storage and utilization, and lipid cytoprotection. Biochimie. 2014;96:96–101.
12. Qiu B, Ackerman D, Sanchez DJ, Li B, Ochocki JD, Grazioli A, et al. HIF2α-dependent lipid storage promotes endoplasmic reticulum homeostasis in clear-cell renal cell carcinoma. Cancer Discov. 2015;5:652–67.
13. Yang WS, Stockwell BR. Ferroptosis: death by lipid peroxidation. Trends Cell Biol. 2016;26:165–76.
14. Cao JY, Dixon SJ. Mechanisms of ferroptosis. Cell Mol Life Sci. 2016;73:11–2.
15. Silke O, Shah R, Li B, Angeli JP, Griesser M, Conrad M, et al. On the mechanism of cytoprotection by Ferrostatin-1 and Liproxstatin-1 and the role of lipid peroxidation in ferroptotic cell death. ACS Cent Sci. 2017;3:232–43.
16. Doll S, Proneth B, Panzilius E, Kobayashi S, Ingold I, et al. ACSL4 dictates ferroptosis sensitivity by shaping cellular lipid composition. Nat Chem Biol. 2017;13:91–8.
17. Migita T, Takayama KI, Obinata D, Ikeda K, Soga T, et al. ACSL3 promotes intratumoral steroidogenesis in prostate cancer cells. Cancer Sci. 2017;108:2011–21.
18. Kelavkar UP, Badr KF. Effects of mutant p53 expression on human 15-lipoxygenase-promoter activity and murine 12/15-lipoxygenase gene expression: evidence that 15-lipoxygenase is a mutator gene. Proc Natl Acad Sci USA. 1999;96:4378–83.
19. Tian R, Zuo X, Jaoude J, Mao F, Colby J, Shureiqi I. ALOX15 as a suppressor of inflammation and cancer: Lost in the link. Prostaglandins Other Lipid Mediat. 2017;132:77–83.
20. Sak ME, Alanbay I, Rodriguez A, Gokaslan T, Borahay M, Shureiqi I, et al. The role of 15-lipoxygenase-1 expression and its potential role in the pathogenesis of endometrial hyperplasia and endometrial adenocarcinomas. Eur J Gynaecolncol. 2016;37(1):36–40.
21. Wang W, Zhang P, Li L, Chen Z, Bai W, Liu G et al. ATD: a comprehensive bioinformatics resource for deciphering the association of autophagy and diseases. Database (Oxford). 2018;2018:bay093. https://doi.org/10.1093/database/bay093.
22. Muhammad JS, Nanjo S, Ando T, Yamashita S, Maekita T, Ushijima T, et al. Autophagy impairment by *Helicobacter pylori*-induced methylation silencing of MAP1LC3Av1promotes gastric carcinogenesis. Int J Cancer. 2017;140:2272–83.
23. Sorrentino A, Federico A, Rienzo M, Gazzerro P, Bifulco M, Ciccodicola A, et al. PR/SET domain family and cancer: novel insights from the Cancer Genome Atlas. Int J Mol Sci. 2018;19:3250 **(Epub ahead of print)**.
24. Fog CK, Asmar F, Côme C, Jensen KT, Johansen JV, Kheir TB, et al. Loss of PRDM11 promotes MYC-driven lymphomagenesis. Blood. 2015;125:1272–8.
25. Dhanoya A, Wang T, Keshavarz-Moore E, Fassati A, Chain BM. Importin-7 mediates nuclear trafficking of DNA in mammalian cells. Traffic. 2013;14:165–75.
26. Laurila E, Vuorinen E, Savinainen K, Rauhala H, Kallioniemi A. KPNA7, a nuclear transport receptor, promotes malignant properties of pancreatic cancer cells in vitro. Exp Cell Res. 2014;322:159–67.